Published in final edited form as:
Nature. 2010 October 21; 467(7318): 991–994. doi:10.1038/nature09408.

Structure of a Cation-bound Multidrug and Toxic Compound Extrusion Transporter

Xiao He, **Paul Szewczyk**, **Andrey Karyakin**, **Mariah Evin**, **Wen-Xu Hong**, **Qinghai Zhang**, and **Geoffrey Chang**[†]
Department of Molecular Biology, The Scripps Research Institute, 10550 N. Torrey Pines Rd, CB105, La Jolla CA 92037

Abstract

Transporter proteins from the multidrug and toxic compound extrusion (MATE)[1] family play vital roles in metabolite transport in plants[2-3], directly affecting crop yields worldwide[4]. MATE transporters also mediate multidrug resistance (MDR) in bacteria and mammals[5], modulating the efficacy of many pharmaceutical drugs used in the treatment of a variety of diseases[6-9]. MATE transporters couple substrate transport to electrochemical gradients and are the only remaining class of MDR transporters whose structure has not been determined[10]. Here we report the x-ray structure of the MATE transporter NorM from *Vibrio cholerae* determined to 3.65 Å, revealing an outward-facing conformation with two portals open to the outer leaflet of the membrane and a unique topology of the predicted 12 transmembrane helices distinct from any other known MDR transporter. We also report a cation-binding site in close proximity to residues previously deemed critical for transport[11]. This conformation likely represents a stage of the transport cycle with high-affinity to monovalent cations and low-affinity to substrates.

Cellular export of toxins and substrates is a fundamental life process, and members of the MATE family represent the last class of multidrug resistance (MDR) transporters to be structurally characterized. MATE transporters are involved in a variety of important biological functions across all kingdoms of life. In plants, MATE transporters are highly prevalent with 58 paralogues found in *Arabidopsis thaliana*[12] and secrete a diverse range of secondary metabolites as a defense against herbivores and microbial pathogens[3,5]. Additionally, plant MATE transporters play an important role in tolerance towards phytotoxic aluminum in acidic soils, a major limitation of crop production in 50% of the world's arable land[4]. In mammals, they export a structurally diverse array of xenobiotic cations in the liver and kidney, influencing the plasma concentrations of many drugs including metformin, a widely prescribed Type 2 diabetes medication, thereby mitigating therapeutic efficacy[8-9]. Bacterial MATE transporters function primarily as xenobiotic efflux pumps and can confer resistance to tigecycline, a new glycylcycline class antibiotic

[†]To whom correspondence should be addressed: gchang@scripps.edu, Telephone: (858) 784-9490 Fax: (858) 784-9985.

Full Methods and any associated references are available in the Supplementary Information section of this manuscript.

Author Contributions. X.H., P.S., A.K., and G.C. designed the experiments and wrote the manuscript. X.H., P.S., A.K., and R.E. performed experiments. W.H. and Q.Z. did chemical synthesis.

Coordinates and structure factors for the structures reported here are available from the Protein Data Bank with accession codes 3MKT and 3MKU.

The authors declare no competing financial interests.

developed to overcome methicillian-resistant and vancomycin-resistant *Staphylococcus aureus*[6-7].

MATE transporters use either H^+ or Na^+ gradients across the membrane to drive substrate export, although the coupling mechanism is not well understood. All MATE proteins share ~40% protein sequence similarity[5] (Fig. S1a), suggesting an overall conserved structure and transport function. To provide a basis for understanding the function of MATE transporters, we present two x-ray structures (Fig. 1) of NorM from *V. cholerae* (NorM-VC) with and without rubidium (Rb^+) using protein purified in n-dodecyl-β-D-maltopyranoside, and crystallized with n-nonyl-β-glucopyranoside (β-NG) and a novel facial amphiphile[13], 3*α*-hydroxy-7*α*,12*α*-bis[(*β*-D-maltopyranosyl)ethyloxy] cholane (FA-231) as additives by methods described previously[14]. Although nearly identical, the NorM-VC apo-structure was solved to a higher resolution at 3.65 Å. The structure reveals a novel topology distinct from all other MDR transporter families[15-19]. This outward-facing conformation also presents a monovalent cation-binding site within the internal cavity. NorM-VC retains transport activity in *Escherichia coli* (Fig. S2) and purified NorM-VC protein binds MATE substrates[5] (Fig. S3; Table S1).

The structure of NorM-VC spans ~50 Å in the plane of the lipid bilayer and is arranged as two bundles of six transmembrane helices (TMs 1-6 and TMs 7-12) forming a large internal cavity open to the extracellular space (Fig. 1). The two halves are related by an intramolecular 2-fold, likely a result of gene duplication as reflected within its primary sequence. A cytoplasmic loop (residues 218-232 between TMs 6 and 7) connects the two halves, as also seen in transporters of the Major Facilitator Superfamily (MFS)[19-21], while the initial helix of each half (TM 1 and TM7) are preceded by a helical extension (residues 2-18, and 233-247) from the inner membrane leaflet side. An additional helix (residues 450-461) after TM12 is nestled under the cytoplasmic side of TM11. The model was obtained as described in Supplementary Information (Fig. S4), refined (Table S2), and verified by multiple $F_{obs} - F_{calc}$ simulated annealing omit maps (Figs. S5-S6). The topology and structural correctness of the model was validated using a series of 16 mercury-labeled single cysteine mutant crystals (Figs. 2a, b, S1a, S7–S8; Table S3). Two structurally similar NorM-VC molecules (NorM1 and NorM2) constitute the asymmetric unit allowing independent verification of the position and identity for each mercury-labeled cysteine residue (Fig. S8).

The topology of NorM-VC is unique amongst all known transporters and unlike other 12 TM transporters such as those of the MFS, no TM-helices intersect the space defined by any cluster of three consecutive helices within each bundle (Fig. 2c, d). For example, in the MFS, TM1 intersects TMs 4-6. Likewise, TM7 intersects TMs 10-12. No such helical arrangement is seen in NorM. Two non-equivalent portals, formed by TMs 1 and 8 on one side and TMs 2 and 7 on the other, open within the lipid bilayer allowing the expulsion of substrates directly to the outer membrane leaflet or the extracellular space (Figs. 3 and S9). Within the lipid bilayer, the portals are maximally ~12 Å wide, sufficient to accommodate substrate passage. The volume of the internal cavity embedded within the lipid bilayer is ~4,300 $Å^3$ (Fig. S10), approximately four times larger than the binding pockets of the transcription MDR regulators xPXR and BmrR[22-23], and nearly two thirds that of ABC exporters Pgp or MsbA[15,17]. Residues facing the internal cavity are both relatively conserved and contributed by all TM helices except for TMs 3 and 9, which are located at the periphery in this conformation (Figs. 1 and S11). Of the 91 residues facing the cavity, 57 are hydrophobic, 14 are aromatic, 20 are polar, and 5 are charged. Nine aromatic residues are clustered in the c-terminal half of the internal cavity (Table S4).

In the internal cavity, we observed the binding of Rb^+ and also cesium (Cs^+) ions, which are heavier alkali metal analogs of sodium more easily visualized by x-ray crystallography (Figs. 4a, b)[14]. The cation binding site of NorM-VC is composed of residues from TMs 7, 8, and 10-12 (Table S4), a fundamentally different topology then found in members of the MFS family (Fig. 2c, d). Previous studies have identified three conserved acidic residues that are critical for transport function in NorM from *V. parahaemolyticus* (NorM-VP)[11], a closely related ortholog of NorM-VC with 76% sequence identity and 86% similarity[24-25]. These residues correspond to D36, E255, and D371 in NorM-VC (D32, E251, and D367 in NorM-VP). In our Rb^+-bound NorM-VC structure, residues E255 and D371 face the internal cavity on the C-terminal half of the molecule and are located near the cation (Fig. 4). For NorM-VP, both of these negatively charged residues are important for transport function as certain mutations at these positions decouple substrate/Na^+ antiport[11]. Like NorM-VP, mutations at residue 255 in NorM-VC affect protein folding and do not express well[11]. Substitution mutations at D371 to alanine or asparagine abolish Rb^+ and Cs^+-binding in the outward-facing conformation (Fig. S12). These findings suggest that these and possibly other surrounding residues are crucial for the recognition and binding of cations from the extracellular space. Mutations of D367 in NorM-VP (D371 in NorM-VC) disrupt transport activity, further suggesting that cation binding at this site plays an important role in the transport cycle[11]. In our outward-facing NorM-VC structure, residue D36 (D32 in NorM-VP) is located in the N-terminal half, far from the C-terminal cation-binding site. We did not observe the presence of either Rb^+ or Cs^+ near D36 and speculate that this residue may play an important role in other conformations.

We propose that the outward-facing conformation of NorM-VC, like other efflux pumps[26-27], represents a state in the transport cycle that has high affinity for monovalent cations (Fig. 4c; step 1), and a lower affinity for substrates. Although the internal cavity is accessible to mercury compounds (Figs. 2a, b and S7), this conformation is not amenable to co-crystallization or soaking with several well-established drugs or transport substrates. Upon cation binding, we propose that NorM-VC undergoes an outward- to inward-facing conformational change more favorable to substrate binding (Fig. 4c; step 2). Herein, cation release/substrate binding could induce a structural change back to the outward-facing conformation[26-27], where the substrate is released into the outer leaflet of the lipid bilayer and/or extracellular space (Fig. 4c; step 3).

The structure of NorM reveals the last known MDR transporter family elucidated by x-ray crystallography. Unlike the Resistance, Nodulation, and Cell-Division (RND) transporter family where an extracellular domain mediates substrate binding, MATE transporters alongside MDR transporters from the ABC, MFS, and SMR families have poly-specific drug binding sites composed of TM helices within the lipid bilayer[15-17,19]. Despite wide primary sequence divergence, extraction and expulsion of substrates directly from the inner to the outer membrane leaflet through portals facing the lipid bilayer (Fig. 4c) may be a common theme for these transporter families. The shared V-shaped conformations suggests this may be the case, providing a molecular basis for hydrophobic/amphipathic substrate transport.

Methods Summary

Crystallization and structure determination

NorM-VC protein was recombinantly expressed in *E. coli BL21 DE3* using pET19b, solubilized with n-dodecyl-β-D-maltopyranoside, and purified by Ni-affinity chromatography. Crystals were grown by the sitting drop method in buffer containing D_2O with Tris-HCL, $(NH_4)_2SO_4$, PEG250DME, 0.23% n-nonyl-β-glucopyranoside (β-NG), and 0.02% FA-231. Wild-type and mutant crystals were derivatized by mercury compounds

dissolved in mother liquor. Diffraction data was processed with the programs HKL2000 and MOSFLM. Protein phasing, model building, and crystallographic refinement were achieved using the programs PHASES, SOLVE/RESOLVE, and CNS v1.2. To verify the identity and position of certain residues as well as characterizing the cation-binding site, NorM-VC wild-type and mutant crystals were soaked with the appropriate compounds and diffraction data collected. Isomorphous difference Fourier maps, calculated using suitable pairs of data sets, were calculated using CNS v1.2 and confirmed the mercury labeling of cysteine residues and the binding of Rb or Cs to the cation-binding site.

Supplementary Material

Refer to Web version on PubMed Central for supplementary material.

Acknowledgments

We thank the contribution of Dr. Y. Yin for initial clones of NorM. We thank CLS, SSRL, ALS, and APS. This work was supported by grants from the NIH GM70480 (GC) and GM73197 (QZ), the Beckman Foundation, the Skaggs Chemical Biology Foundation.

References

1. Brown MH, Paulsen IT, Skurray RA. The multidrug efflux protein NorM is a prototype of a new family of transporters. Mol Microbiol. 1999; 31:394–395. [PubMed: 9987140]
2. Magalhaes JV, et al. A gene in the multidrug and toxic compound extrusion (MATE) family confers aluminum tolerance in sorghum. Nat Genet. 2007; 39:1156–1161. doi:ng2074 [pii]. 10.1038/ng2074 [PubMed: 17721535]
3. Morita M, et al. Vacuolar transport of nicotine is mediated by a multidrug and toxic compound extrusion (MATE) transporter in Nicotiana tabacum. Proc Natl Acad Sci U S A. 2009; 106:2447–2452. doi:0812512106 [pii]. 10.1073/pnas.0812512106 [PubMed: 19168636]
4. Wood, S.; S, KL.; Scherr, SJ. Pilot analysis of global ecosystems : agroecosystems. Vol. xii. World Resources Institute; Washington, D.C.: 2000. p. 110
5. Omote H, Hiasa M, Matsumoto T, Otsuka M, Moriyama Y. The MATE proteins as fundamental transporters of metabolic and xenobiotic organic cations. Trends in Pharmacological Sciences. 2006; 27:587–593. [PubMed: 16996621]
6. Kaatz GW, McAleese F, Seo SM. Multidrug Resistance in Staphylococcus aureus Due to Overexpression of a Novel Multidrug and Toxin Extrusion (MATE) Transport Protein. Antimicrob Agents Chemother. 2005; 49:1857–1864.10.1128/aac.49.5.1857-1864.2005 [PubMed: 15855507]
7. McAleese F, et al. A Novel MATE Family Efflux Pump Contributes to the Reduced Susceptibility of Laboratory-Derived Staphylococcus aureus Mutants to Tigecycline. Antimicrob Agents Chemother. 2005; 49:1865–1871.10.1128/aac.49.5.1865-1871.2005 [PubMed: 15855508]
8. Becker ML, et al. Genetic variation in the multidrug and toxin extrusion 1 transporter protein influences the glucose-lowering effect of metformin in patients with diabetes: a preliminary study. Diabetes. 2009; 58:745–749. doi:db08-1028 [pii]. 10.2337/db08-1028 [PubMed: 19228809]
9. Tsuda M, et al. Targeted Disruption of the Multidrug and Toxin Extrusion 1 (Mate1) Gene in Mice Reduces Renal Secretion of Metformin. Mol Pharmacol. 2009; 75:1280–1286.10.1124/mol.109.056242 [PubMed: 19332510]
10. Saier MH Jr, Tran CV, Barabote RD. TCDB: the Transporter Classification Database for membrane transport protein analyses and information. Nucl Acids Res. 2006; 34:D181–186.10.1093/nar/gkj001 [PubMed: 16381841]
11. Otsuka M, et al. Identification of essential amino acid residues of the NorM Na+/multidrug antiporter in Vibrio parahaemolyticus. J Bacteriol. 2005; 187:1552–1558. doi:187/5/1552 [pii]. 10.1128/JB.187.5.1552-1558.2005 [PubMed: 15716425]

12. Hvorup RN, et al. The multidrug/oligosaccharidyl-lipid/polysaccharide (MOP) exporter superfamily. Eur J Biochem. 2003; 270:799–813.10.1046/j.1432-1033.2003.03418.x [PubMed: 12603313]
13. Zhang QH, et al. Designing facial amphiphiles for the stabilization of integral membrane proteins. Angew Chem Int Edit. 2007; 46:7023–7025.10.1002/anie.200701556
14. Supplemental materials associated with this publication Materials and Methods Section.
15. Aller SG, et al. Structure of P-glycoprotein reveals a molecular basis for polyspecific drug binding. Science. 2009; 323:1718–1722. doi:323/5922/1718 [pii]. 10.1126/science.1168750 [PubMed: 19325113]
16. Chen YJ, et al. X-ray structure of EmrE supports dual topology model. Proc Natl Acad Sci U S A. 2007; 104:18999–19004. doi:0709387104 [pii]. 10.1073/pnas.0709387104 [PubMed: 18024586]
17. Ward A, Reyes CL, Yu J, Roth CB, Chang G. Flexibility in the ABC transporter MsbA: Alternating access with a twist. Proc Natl Acad Sci U S A. 2007; 104:19005–19010. doi: 0709388104 [pii]. 10.1073/pnas.0709388104 [PubMed: 18024585]
18. Murakami S, Nakashima R, Yamashita E, Yamaguchi A. Crystal structure of bacterial multidrug efflux transporter AcrB. Nature. 2002; 419:587–593. nature01050 [pii]. 10.1038/nature01050 [PubMed: 12374972]
19. Yin Y, He X, Szewczyk P, Nguyen T, Chang G. Structure of the multidrug transporter EmrD from Escherichia coli. Science. 2006; 312:741–744. doi:312/5774/741 [pii]. 10.1126/science.1125629 [PubMed: 16675700]
20. Abramson J, et al. Structure and mechanism of the lactose permease of Escherichia coli. Science. 2003; 301:610–615. [PubMed: 12893935]
21. Huang YF, Lemieux MJ, Song JM, Auer M, Wang DN. Structure and mechanism of the glycerol-3-phosphate transporter from Escherichia coli. Science. 2003; 301:616–620. [PubMed: 12893936]
22. Zheleznova EE, Markham PN, Neyfakh AA, Brennan RG. Structural basis of multidrug recognition by BmrR, a transcription activator of a multidrug transporter. Cell. 1999; 96:353–362. [PubMed: 10025401]
23. Watkins RE, et al. The human nuclear xenobiotic receptor PXR: Structural determinants of directed promiscuity. Science. 2001; 292:2329–2333. [PubMed: 11408620]
24. Altschul SF, et al. Gapped BLAST and PSI-BLAST: a new generation of protein database search programs. Nucleic Acids Res. 1997; 25:3389–3402. gka562 [pii]. [PubMed: 9254694]
25. Altschul SF, et al. Protein database searches using compositionally adjusted substitution matrices. FEBS J. 2005; 272:5101–5109. doi:EJB4945 [pii]. 10.1111/j.1742-4658.2005.04945.x [PubMed: 16218944]
26. Jardetzk O. Simple Allosteric Model for Membrane Pumps. Nature. 1966; 211:969–&. [PubMed: 5968307]
27. Law CJ, Maloney PC, Wang DN. Ins and outs of major facilitator superfamily antiporters. Annu Rev Microbiol. 2008; 62:289–305.10.1146/annurev.micro.61.080706.093329 [PubMed: 18537473]

Figure 1. NorM-VC model

a, Front and **b**, back views of NorM-VC, with extracellular and cytoplasmic sides indicated. Stereo views presented in Fig. S1b. **c**, Extracellular view, with TM helices 1-12 marked. The internal cavity opens to the extracellular space and is occluded on the cytoplasmic side. The molecule is colored using a rainbow gradient from the N- (blue) to C-terminus (red).

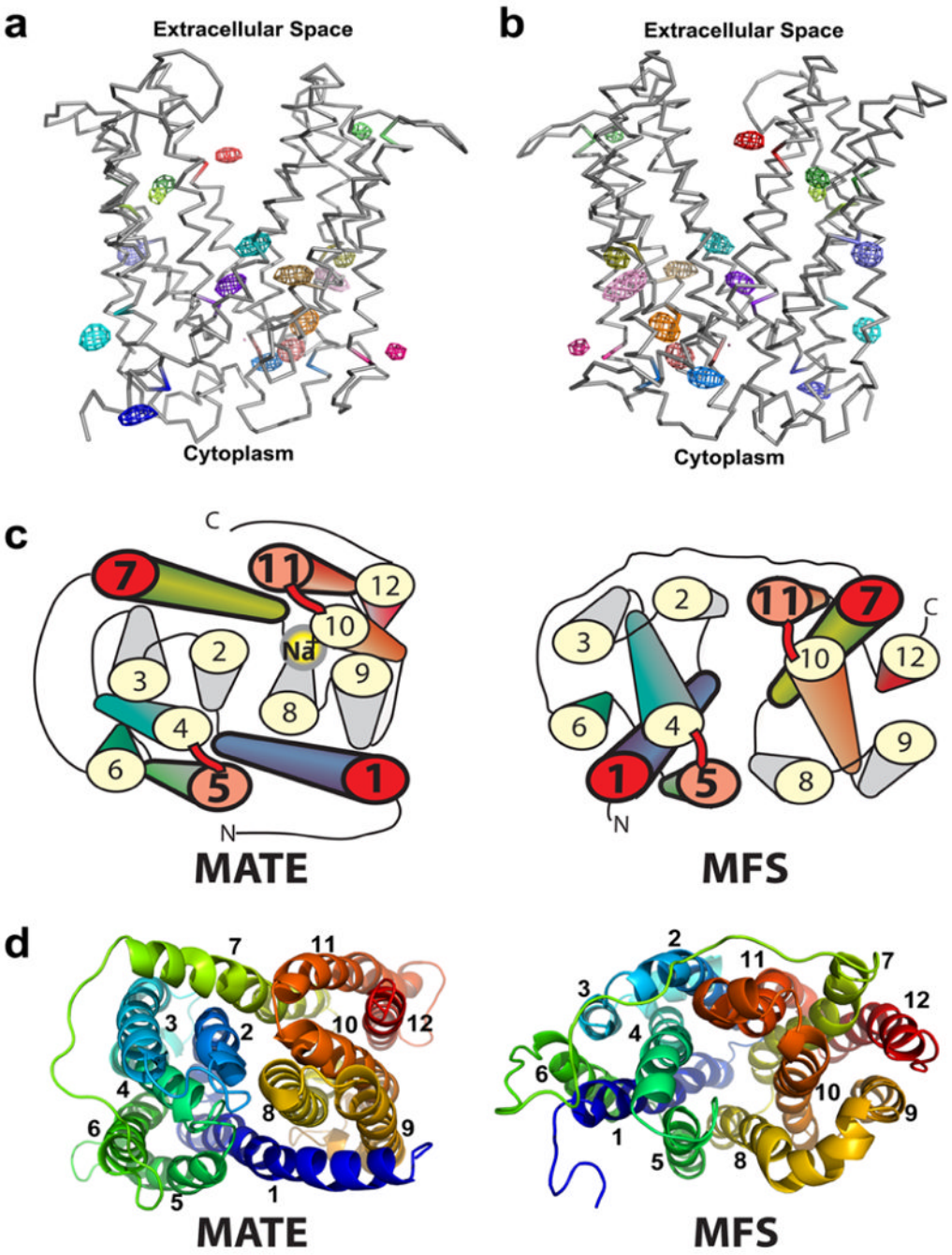

Figure 2. Validation of the NorM-VC model, showing the positions of the 16 mercury-labeled cysteine mutants

a, Front and **b**, back views of a NorM-VC monomer (gray backbone) with isomorphous difference Fourier peaks, and mutated residues colored. Stereo views presented in Fig. S7. **c**, Topological comparison between MATE (left) and MFS (right) transporters from the cytoplasmic side. The C-terminal helix (residues 450-461) is removed for clarity and position of cation (Na^+) is indicated. In MATE transporters; TM1 is between TMs 5 and 8, and TM7 is between TMs 3 and 11. The portals facing the membrane are formed between TMs 1 and 8, and TMs 2 and 7. In contrast, the MFS has TM1 between TMs 4, 5 and 6.

Likewise, TM7 is between TMs 10, 11 and 12. **d**, x-ray structures of NorM, and the MFS transporter EmrD[19].

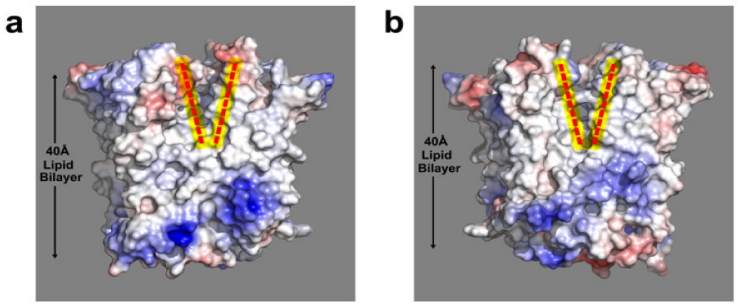

Figure 3. Electrostatic potential surface representation of NorM-VC

a, Views of the portals formed by TMs 1 and 8 and **b**, TMs 2 and 7, opening to the outer membrane leaflet highlighted and marked by dashed lines (yellow). The same views are shown in Fig. 1a, b. The surface of NorM is colored by amino acid residue charge ranging from blue (positive) to red (negative). Hydrophobic and aromatic residues are colored in white. TM regions embedded within the lipid bilayer are indicated. Stereo views are presented in Fig. S9.

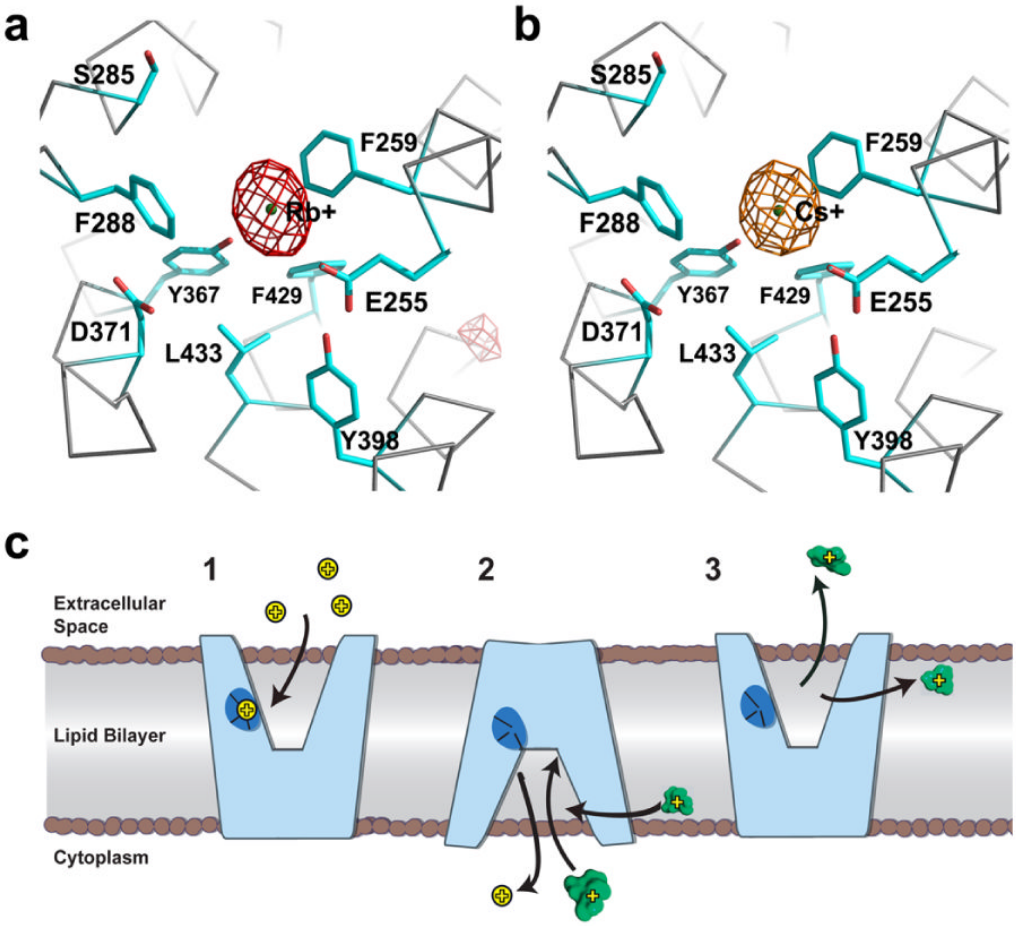

Figure 4. The cation-binding site of NorM-VC and mechanism of transport

a, Cation-binding site superimposed with isomorphous difference Fourier map calculated between Crystal 2 (containing Rb^+) and Crystal 3 (native) (Table S3), revealing a Rb^+ peak at 5.5 σ (red mesh). **b**, A 5.0 σ peak (orange mesh) revealing binding of Cs^+ in the same view as **a**, calculated between Crystal 4 (containing Cs^+) and Crystal 3 (native). Stereo views presented in Fig. S12. **c**, Proposed transport mechanism: In the outward-facing conformation, cation (yellow) binds at a conserved site (blue oval; step 1). Cation binding induces structural changes to the inward-facing conformation (step 2), which is competent to bind substrate (organic cation in green) from the inner membrane leaflet or cytoplasm. Substrate binding causes structural changes back to the outward-facing conformation (step 3), allowing export and cation binding.